Batteries & Supercaps

Research Article
doi.org/10.1002/batt.202400298

Chemistry Europe
European Chemical Societies Publishing

www.batteries-supercaps.org

New Insights Into Zinc Passivation Through Operando Measured Zincate Concentrations

David Fuchs,[a] Christoph Müller,[b] Mandy Schaffeld,[a] Falko Mahlendorf,*[a] and Harry E. Hoster[a]

We present a detailed analysis of the behavior of a new zinc-air flow cell. This system offers several unique insights into the zinc electrochemistry. Due to the constant slurry flow, concentration gradients are completely destroyed every few seconds and therefore negligible and it is possible to take samples from the anode without interrupting the discharge process. To clarify the underlying processes, the potential of the zinc electrode, the zincate concentration (by titration) and the zinc-particles (by SEM) were analyzed. These measurements offer the unique opportunity to distinguish between thermodynamic and kinetic contributions to the cell voltage. We found, that in this system zinc passivation, is caused by a critical zincate concentration and the steep increase of the cell potential is a kinetic effect, caused by partial passivation. The key factor for passivation, which limits the capacity to 82 mAh g_{zinc}^{-1} or 41 mAh g_{slurry}^{-1}, is the nucleation of ZnO before the critical zincate concentration is reached. This allows capacities of up to 420 mAh g_{zinc}^{-1} or 210 mAh g_{slurry}^{-1}. These results are therefore not only essential for a further increase of the practical capacity of the system but also offer unique insights in the zinc electrochemistry.

Introduction

Due to the increasing demand for energy storage systems alternatives for the currently dominating lithium-ion batteries, so called beyond lithium-ion systems, are investigated with renewed effort. Zinc-air cells are one of the best developed systems in this group. These batteries have been commercialized as alkaline, non-rechargeable systems long ago[1] and there are numerous descriptions of different cells in literature, e.g.,.[2–13] Currently, zinc-air flow cells are investigated for stationary applications mostly. Compared to other stationary systems, zinc-air cells have a high theoretical capacity of 3700 Ah L^{-1}. The practical capacity of zinc-air flow cells is mainly limited by electrolyte/zinc ratio and the zinc usage. For a detailed overview of zinc-air flow batteries with zinc suspension electrodes see.[14] As in most zinc-air flow cells,[2–13] the zinc is completely dissolved in the discharged state, the electrolyte/zinc ratio is restricted by the amount of ZnO which can be electrochemically dissolved. Due to the large amounts of electrolyte needed for complete zinc dissolution, the theoretical capacity of these systems is relatively low (up to 295 g L^{-1} zinc, or 240 Ah L^{-1}[3]). It should be noted that pure KOH solutions are easily electrochemically supersaturated (relative to the solubility limit measured by dissolving ZnO in KOH),[15–16] but still at least 1 L electrolyte is required to dissolve 300 g of zinc.[3] One approach to overcome these limitations would be the usage of a zinc suspension electrode (zinc-slurry). In this zinc-slurry, the zincate solubility limit is exceeded, which could lead to much higher energy densities. Then, the energy density of the system is mainly restricted by zinc passivation. The corresponding passivation mechanisms of zinc in alkaline solutions are still not completely understood. Here, we will give a brief overview, for more details we recommend corresponding review articles, e.g..[17] Generally, passivation is caused by the formation of an insoluble layer of oxidation products which prevents further oxidation of the zinc electrode. In concentrated alkaline solutions, this layer is known to consist mainly of ZnO.[18] The different mechanisms for zinc passivation published in literature can be divided in two groups. One set of theories[19–23] describes passivation as a process that starts once a critical zinc potential is exceeded, while the other set[15,24–27] identifies a critical zincate concentration as the starting point of passivation.

According to Liu et al.,[15] the first group which related passivation directly to a critical zincate concentration, there are three stages of zinc oxidation in alkaline electrolytes. During these stages the reactions in Equation 1-1 to Equation 1-3 occur.

Phase I

$$Zn + 4\ OH^- \rightarrow Zn(OH)_4^{2-} + 2\ e^- \quad (1\text{-}1)$$

[a] Dr. D. Fuchs, M. Schaffeld, Dr. F. Mahlendorf, Prof. Dr. H. E. Hoster
Energy Technology
University Duisburg-Essen
Lotharstraße 1, 47057 Duisburg
Germany
E-mail: david.fuchs@uni-due.de

[b] Dr. C. Müller
GRILLO-Werke Aktiengesellschaft
Weseler Straße 1, 47169 Duisburg
Germany

Supporting information for this article is available on the WWW under https://doi.org/10.1002/batt.202400298

Research Article
doi.org/10.1002/batt.202400298
Chemistry Europe
European Chemical Societies Publishing

Phase II

$$Zn + 4\ OH^- \rightarrow Zn(OH)_4^{2-} + 2\ e^- \quad (1\text{-}1)$$

$$Zn(OH)_4^{2-} + \square \rightarrow ZnO\ (type\ I) + H_2O + 2\ OH^- \quad (1\text{-}2)$$

Phase III

$$Zn + 2\ OH^- \rightarrow ZnO\ (type\ II) + H_2O + 2\ e^- \quad (1\text{-}3)$$

In the first phase of the zinc oxidation only soluble oxidation products are produced, mainly zincate but also polynuclear species are possible.[16] When the zincate concentration reaches a critical concentration and an appropriate crystallation site (□, seeding crystal or ZnO surface) is available, ZnO starts to precipitate as type I ZnO (Equation 1-2). This type of ZnO does not passivate the zinc electrode, so the film can reach a thickness of several μm.[28] This reaction is reversible, at zincate concentrations below the solubility limit the equilibrium of this reaction is on the zincate side. The type I ZnO film reduces the diffusion of OH^--ions to the surface of the electrode. Once there are insufficient OH^--ions to form zincate, type II ZnO is produced according to Equation 1-3.[15] This type of zinc oxide prevents the further oxidation of zinc and causes passivation of the electrode. If there is a forced electrolyte convection, there may be no type I ZnO formation before the passivation of the electrode.[29–30]

The other set of theories[19–23] claim that passivation occurs when a critical potential is exceeded. When this potential is reached, type II ZnO-clusters are nucleated. Passivation occurs when these clusters cover the whole zinc surface.

As mentioned above, the passivation mechanisms of zinc in different alkaline electrolytes have been addressed in several publications. Only a few groups investigated the behavior of zinc electrodes in electrolytes with zincate concentrations above the solubility limit.[16,25,27,31–35] Although many battery systems, e.g.[3,5,7–8] operate in this concentration range, the passivation mechanisms at these high zincate concentrations are still not fully understood. But none of these publications describes the passivation process of pumped slurry electrodes. The conditions in these cells differ from the conditions of the cells described in literature in several important ways. The first significant difference is that in these cells the whole anode is replaced periodically. Secondly, the amount of electrolyte in the slurry cell is much lower than in the cells described in literature. This low amount of electrolyte leads to much higher zincate concentrations in the bulk of the electrolyte than in the electrolytes investigated in literature.

Here, we present a comprehensive analysis of the passivation behaviour of a complete lab-scale zinc-air flow battery. We analysed the changes in cell voltage, potential of the zinc electrode and the composition of the zinc-slurry, especially the zincate concentration obtained by titration with EDTA, during galvanostatic discharge at varying current densities and electrolyte concentrations.

Experimental

Zinc-Slurry

The zinc-slurries were prepared using battery zinc powder (zp001), ZnO, Carbopol ® 941, KOH (technical grade, 86% purity) and deionized water. All chemicals were supplied by

Grillo-Werke AG, Germany, and used as received. The volumetric zinc content of all slurries was 15 vol.–%, due to different electrolyte densities this value corresponds to different gravimetrical zinc contents. The slurry based on 7 mol L^{-1} KOH contained 50 wt.–% zinc, 0.5 wt.-% Carbopol and 49.5 wt.–% electrolyte (7 mol L^{-1} KOH, 0.48 mol L^{-1} ZnO). The slurry based on 12 mol L^{-1} KOH contained 47 wt.–% zinc, 0.5 wt.-% Carbopol and 52.5 wt.–% electrolyte (12 mol L^{-1} KOH, 0.48 mol L^{-1} ZnO). The volumetric zinc content of both slurries is 15 vol.-%. Depth-of-Discharge (DoD) value refer to the overall Zn amount, i.e., 100% DoD would be the point where no metallic Zn is left.

Cell Construction

The testing cell had total dimensions of 250 mm x 180 mm×55 mm. The anodic current collector and the cathode had an area of 100 mm×100 mm. All current densities are given relative to this area. The gap between anode and cathode was 2 mm. During discharge, the gap was completely filled with zinc-slurry. In this gap was a sealed (with Celgard ® 5550) capillary, which led to a reversible hydrogen electrode (RHE) reference electrode (Hydroflex®, Gaskatel, Germany). The slurry was separated from the cathode using a microporous separator (Celgard ® 5550, Azelis Deutschland GmbH, Germany). The air electrode was a commercially available Oxygen Depolarized Cathode from Covestro Deutschland AG, Germany.

In Figure 1 a we show a schematic representation of the battery system used in this work. The pump is upstream of the battery cell. The slurry was pumped through the system using a Verdeflex ® Rapid R6 (Verder Liquids B.V., Netherlands). Downstream of the testing cell was a manual valve, which could divert the slurry stream to a separate flask. It was therefore possible to take slurry samples without interrupting the discharge process. The flow rate of the slurry was 170 mL min^{-1}. The battery system was filled with 450–550 g (200–250 mL) of zinc-slurry, depending on the estimated amount of slurry samples taken during discharge.

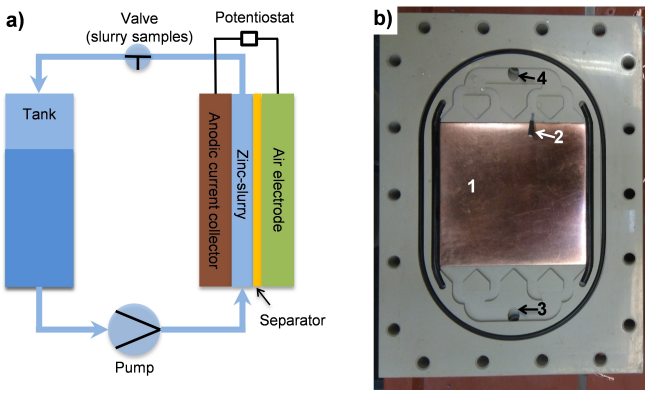

Figure 1. Schematic representation of the battery system (tank, pump, cell) (a) and picture of the slurry half-cell (b) with copper current collector (1), capillary of reference electrode (2), slurry inlet (3) and outlet (4).

Research Article
doi.org/10.1002/batt.202400298
Chemistry Europe
European Chemical Societies Publishing

Figure 1 b shows the slurry half-cell of the battery cell. The copper current collector (CW08A) had an area of 100 cm^2, all current densities in this publication are given respective this area. The capillary for the reference electrode (2) was placed between current collector and separator. The slurry was pumped upwards from the inlet (3) to the outlet (4). During discharge, approx. 20 mL (the volume between anodic current collector and separator) or approx. 44 g of the zinc slurry was electrochemically active. The rest of the slurry was in the tubing system or the tank. the pumping speed was sufficient to completely replace the slurry every 7 s.

The galvanostatic discharges were controlled using a VMP3 potentiostat with an 80A booster (BioLogic ® Science Instruments GmbH, Germany) using EC-Lab 11.31 software.

The DoD was calculated by dividing the transferred charge by the theoretical charge of the total amount of zinc-slurry in the system.

Analysis of the Zinc-Slurry

To determine the zincate concentration in the liquid phase of the zinc-slurry, the whole slurry was diverted at the valve in figure 1a. The resulting slurry samples were divided into 4 sub-samples of approx. 0.5 g and analysed. The given standard deviation includes sample preparation and titration. Each sub-sample was extracted using 1 mol L^{-1} KOH. The resulting solution contained a liquid and a solid phase. The liquid phase consisted of the extracting solution, the liquid phase of the slurry and at high depths of discharge (DoD) of ZnO precipitated from the bulk of the slurry. After the sedimentation of the ZnO, this phase was used for zincate analysis. The solid phase was washed with deionised water, ethanol, then dried for 24 h under ambient conditions and weighed. The mass of the liquid phase was determined by subtracting the mass of the solid phase from the mass of the slurry sample and converted to a volume by using the density of 7 mol L^{-1} KOH, calculated according to Gilliam et al.[36] (see supplementary information for more details).

Zincate concentrations were measured by titrating 1 mL of the KOH used for extraction with 0.02 mol L^{-1} EDTA (Disodium ethylenediaminetetraacetic acid, 99.0–101.0% purity, Merck, Germany) using Erio-T (sodium-3-hydroxy-4-(2-hydroxy-1-naphthylazo)-7-nitro-1-naphthalin-sulfonate, ACS indicator grade, Merck, Germany). All chemicals were used as received. The titration was performed only once. This method does not provide any information of the present zinc species, the term zincate concentration is used because zincate is the dominating complex in high concentrated KOH solutions.[37]

The techniques used to show the passivating ZnO in literature (e.g. optical microscopy,[19,23] Raman spectroscopy,[18] Atom-Emission-Spectroscopy[22]) are not useful in our system, because the electrochemical oxidation takes place in pits and caverns of the zinc particles (see supporting information). The passivating layer is too thin (approx. 70 atom layers[19]) to be visible in SEM.

Results and Discussion

In this work, we evaluate whether the passivation mechanisms described in literature for stationary electrodes can describe the passivation mechanisms in pumped slurry electrodes as well. As mentioned in the introduction, the theories described in literature either identified a critical zinc potential[19–23] or a critical zincate concentration[15,24–27] as reason for zinc passivation. Moreover, we tried to verify the reported linear dependency of the critical zincate concentration from the KOH-concentration by investigating two KOH-concentrations (7 and 12 mol L^{-1}).

Cell Voltage and Zinc Potential

Figure 2 depicts the results of galvanostatic discharge of zinc-slurry electrodes with different current densities. The DoDs are given relative to the total zinc mass in the system, the top x-axis in Figure 2 a shows the zincate concentration in the electrolyte when the oxidation proceeds according to Equation 1-1 and ZnO precipitation does not occur. The solubility limit of ZnO is surpassed at approx. 1% DoD, but according to literature,[25,27] it is possible to supersaturate KOH solutions to a concentration which is equal to the KOH concentration divided by two (supersaturation limit). The solubility limit is calculated according to Dirkse[38] and describes the concentration when ZnO and KOH are in equilibrium.

The voltage and potential curves in Figure 2 a show two or three stages of discharge, depending on the current density. In Figure 2 b, this dependency is even more obvious. All cells discharged with a current density of 25 mA cm^{-2} or higher fail

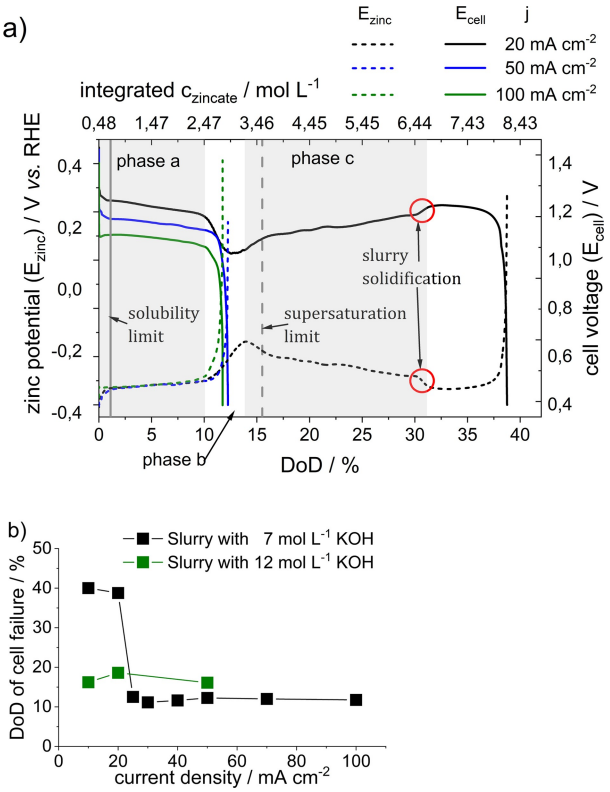

Figure 2. a) Cell voltage (solid lines) and potential of the zinc electrode (dashed lines) of a zinc-air flow cell during galvanostatic discharge with different current densities, x-axis depth of discharge (DoD = $Q/Q_{theor.}$), the top x-axis shows the zincate concentration calculated according to Equation 1-1 (zincate is only reaction product), b) DoD of cell failure of galvanostatic discharges of a zinc-air flow cell as a function of the current density, RE: reversible hydrogen electrode (RHE), slurry electrode with 50 wt.-% zinc, 7 mol L^{-1} KOH and 0.48 mol L^{-1} ZnO, and 47 wt.-% zinc, 12 mol L^{-1} KOH and 0.48 mol L^{-1} ZnO, room temperature, cut-off criterion cell voltage < 0.4 V.

at the end of phase b, only cells discharged with 20 mA cm^{-2} or lower may reach phase c. It is possible to postpone the cell failure at the end of phase b to 16–18% DoD by increasing the KOH concentration to 12 mol L^{-1}.

Phase a

After a short initialization period, all measurements show a virtually linear decrease of cell voltage until about 10% DoD corresponding to an integrated zincate concentration of ~2.5 mol L^{-1}. The dashed lines confirm that the zinc electrode potentials are hardly affected by the current densities. Lower cell voltages at higher current densities are due to the voltage drop at the air electrode, which is a known phenomenon in zinc-air cells (e.g.[2]) and not in scope of this work.

Phase b

Phase b is characterized by a steep voltage drop. At higher current densities (Figure 2 a $\geq$ 50 mA cm^{-2}), the cell voltage drops below the 0.4 V cut-off threshold. The zinc electrode potentials show a steep potential rise at the end of the measurement.

We will show in this paper that the root cause for this potential rise and the following termination of discharge is passivation[15,23,39] of the zinc electrode.

Deeper optical or spectroscopic analysis[18–19,22–23] of the passivation process is not possible in our cell, as we cannot apply the techniques described in literature: our slurry is opaque and the movement of the zinc particles distorts the impedance spectra, especially at low frequencies.[40]

At low current densities ($\leq$ 20 mA cm^{-2}), the rise of the potential of the zinc electrode is slower than at higher current densities and the cell voltage does not reach the cut off criterion. Instead, the cell voltage rises again and the discharge continues.

The potential measurements show the same trends as the voltage curves. At a potential of −340 and −350 mV vs. RHE and a DoD of approx. 10%, the potential of the zinc electrode starts to increase. At high current densities, the slurry electrode passivates, but at low current densities the potential of the zinc electrode reaches a potential of ~−0.2 V vs RHE before it starts to decrease again. This behavior indicates, that in all measurements the zinc electrode starts to passivate, but at low current densities the passivation reaction stops before the electrode is fully passivated and the electrode recovers. As the overpotential is approx. 150 mV higher, than at the point where the passivation reaction started, the reason for passivation cannot be a critical potential. Instead, passivation has to be caused by another effect, which also influences the potential of the zinc electrode – probably a critical zincate concentration.

When the ZnO solubility is increased by using a higher KOH concentration (12 mol L^{-1}), the zinc-slurry passivated at a slightly higher DoD of 16–20% Figure 2b. This is a clear sign, that passivation might be caused by a critical zincate concentration, which depends on the solubility limit of the electrolyte. If zincate is the only reaction product, this concentration is independent from the current density and always reached at the same DoD.

Phase c

This phase of discharge is much longer than the first two phases, but only present in cells discharged with 20 mA cm^{-2} or lower. The cell voltage increases and the potential of the zinc electrode decreases, until at DoDs between 35 and 45% (in the measurement in Figure 2a 35% DoD) the slurry solidifies, and the electrode becomes stationary. Once the slurry flow stops, percolation networks stabilized by Van der Waals forces are formed. These percolation networks increase the slurry conductivity and the cell voltage. The measurements do not stop at this point, instead the slurry inside the cell is discharged until the remaining zinc passivates at DoDs between 40 and 50% (with respect to the total zinc amount of the system). In this case, we consider the cell blockage due to slurry solidification as reason for cell failure. This effect does not always occur at a fixed DoD, but in the range between 35 and 45% DoD. The reasons for slurry solidification will be the scope of another publication.

Measurements of the Zincate Concentration

Passivation is frequently described as a phenomenon caused by a specific (critical) zincate concentration.[15,24–27] We therefore measured the zincate concentration in the liquid phase of the zinc-slurry via titration (EDTA) of samples (2–3 g), taken at selected DoDs. To investigate the influence of the KOH concentration, we analyzed slurries containing 7 and 12 mol^{-} l^{-1} KOH. As all slurries containing 12 mol L^{-1} passivated, we investigated this electrolyte only at a current density of 50 mA cm^{-2} (Figure 3 a). In 7 mol l^{-1} KOH, passivation did not occur at low current densities (Figure 3 a). we therefore chose two current densities (50 and 100 mA cm^{-2}, Figure 3) a where the zinc-slurry passivated at approx. 11% DoD and one current density (16 mA cm^{-2}, Figure 3b) which was low enough to avoid passivation at this DoD.

The discharges in Figure 3a terminate due to passivation and the last sample was taken from the passivated slurry immediately after the end of discharge, while the measurements in Figure 3b were stopped when sample extraction had depleted the slurry inventory.

The black lines in Figure 3 show the expected zincate concentration when zincate is the only reaction product. The values were calculated by adding the amount of electrochemically produced zincate (Faradays law), see Equation 1-1, to the measured starting concentration. We calculated different curves for the two different electrolytes because the starting concentration in 12 mol L^{-1} is a little higher due to self-discharge (all slurries were prepared using an electrolyte containing 0.48 mol L^{-1} ZnO). Measured values lower than the calculated

Research Article
doi.org/10.1002/batt.202400298
Chemistry Europe
European Chemical Societies Publishing

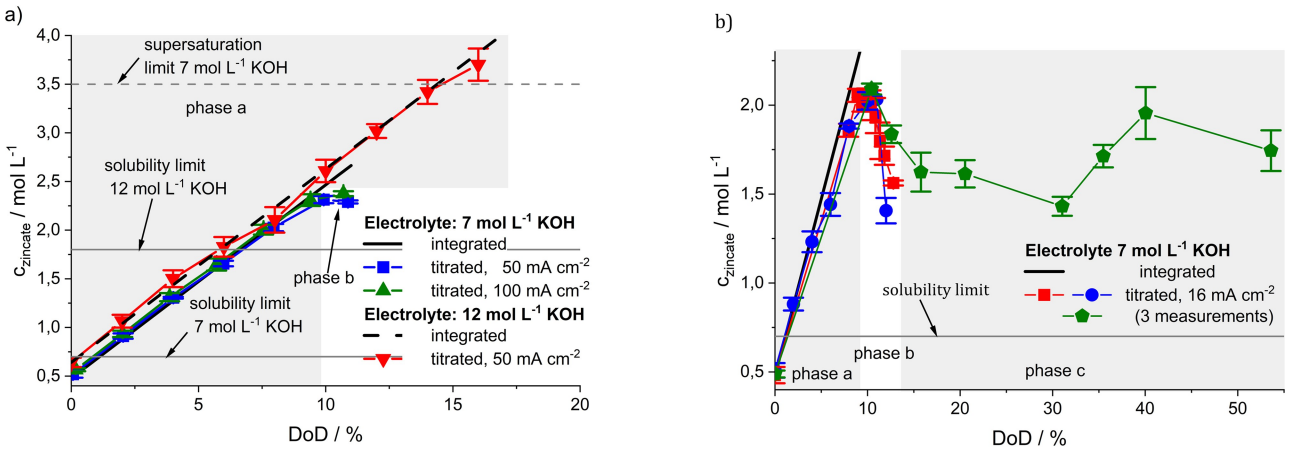

Figure 3. Higher current (50…100 mA cm^{-2}, a) and low current (16 mA cm^{-2}, b) galvanostatic discharge: zincate concentration in the liquid phase of the slurry anode of a zinc-air flow cell; slurry-electrode with 50 wt.-% zinc, 7 mol L^{-1} KOH and 0.48 mol L^{-1} ZnO, and 47 wt.-% zinc, 12 mol L^{-1} KOH and 0.48 mol L^{-1} ZnO, room temperature, cut-off criterion cell voltage <0.4 V; black lines show the concentrations expected from charge integration (Faraday's law) for an oxidation where zincate is the only product. Solubility limits were calculated according to Dirkse,[38] supersaturation limit according to,[24–25] sample preparation and zincate titration using EDTA were repeated 4 times.

values show that ZnO precipitation according to Equation 1-2 (type I ZnO) or passivation according to Equation 1-3 (type II ZnO) occurs. Values higher than the calculated ones would imply self-discharge.

Phase a

The measured zincate concentrations surpass the solubility limits early (∽1 and ∽5% DoD) during discharge and the cell is operated beyond zincate solubility limit for most of the time. This phase lasts until approx. 10% DoD in 7 mol L^{-1} KOH and until cell failure at 16–18% DoD in 12 mol L^{-1} KOH. In Figure 3 a measured and integrated zincate concentration are equal and the SEM-micrographs do not show any signs of ZnO. Therefore, zincate is the only reaction product and ZnO precipitation does not occur. This phase of discharge was first referred to by Liu et al.[15] as "first phase of discharge".

At low current density (Figure 3 b), the titrated zincate concentration starts to be lower than the integrated one already at a DoD of 4%. The extraction solution of the slurry samples becomes turbid at this DoD, which we attribute to ZnO precipitation. There are no distinguishable ZnO crystallites on the zinc particles (SEM imaging of the particles of the sample, see supplementary information, Figures S1 and S2).

Phase a ends when the titrated zincate concentration ceases to rise. At low current densities, phase a ends at a lower zincate concentration of ∽2 mol L^{-1} (Figure 3 b) instead of 2.3 mol L^{-1} (Figure 3 a) at high current densities.

Phase b

During this phase of discharge, the measured zincate concentration in 7 mol L^{-1} KOH remains stable either until the cell fails due to passivation, or the measured zincate concentration starts to decrease. Apparently, the cell failure due to passivation is linked to reaching a certain (critical) zincate concentration: ∽2.3 mol L^{-1} for both measurements with 7 mol L^{-1} KOH and 3.7 mol L^{-1} in 12 mol L^{-1} KOH. As all measurements in Figure 2b (six measurements with 7 mol L^{-1} KOH and three measurements with 12 mol L^{-1} KOH, Figure 2b) passivate at approx. the same DoD, one can conclude that the zincate concentration at the point of passivation does not depend on the current density but rather on the KOH concentration.

Our measured critical zincate concentrations are much lower than the supersaturation limit: the value of 6 mol L^{-1} zincate for 12 mol L^{-1} KOH is beyond the y-axis range. The possible reasons for this behavior are discussed after Figure 4. The main question here is why the zincate concentrations in phase b remain lower at low current densities (Figure 3b).

If the measured zincate concentration is lower than the integrated one, this means that either zincate is removed from the solution (precipitation to type I ZnO Equation 1-2), or the zincate production stops and is replaced by the production of passivating type II ZnO (Equation 1-3), or a combination of both effects. The amount of visible type I ZnO crystallites, freely dispersed and attached to zinc particles, increases from high to low current densities. At 50 mA cm^{-2} they are hardly detectable, whereas at 16 mA cm^{-2} they are clearly visible (see supplementary information, Figure S2b). This means that passivation must have started in phase b at high current densities (50 and 100 mA cm^{-2}).The increasing potential of the zinc electrode in Figure 2 a indicates that some direct oxidation (passivation) also occurs at low current densities. Unfortunately, type II ZnO does not come with morphological features we could identify by SEM (given the intrinsic roughness of our zinc particles).

The nucleation of ZnO in the bulk of the electrolyte is the key enabler for reaching deep discharges (phase c). Surpassing the critical zincate concentration can only be avoided if the chemical ZnO formation out of zincate (Equation 1-2) is at least as fast as the electrochemical zincate formation (Equation 1-1).

Research Article
doi.org/10.1002/batt.202400298
Chemistry Europe
European Chemical Societies Publishing

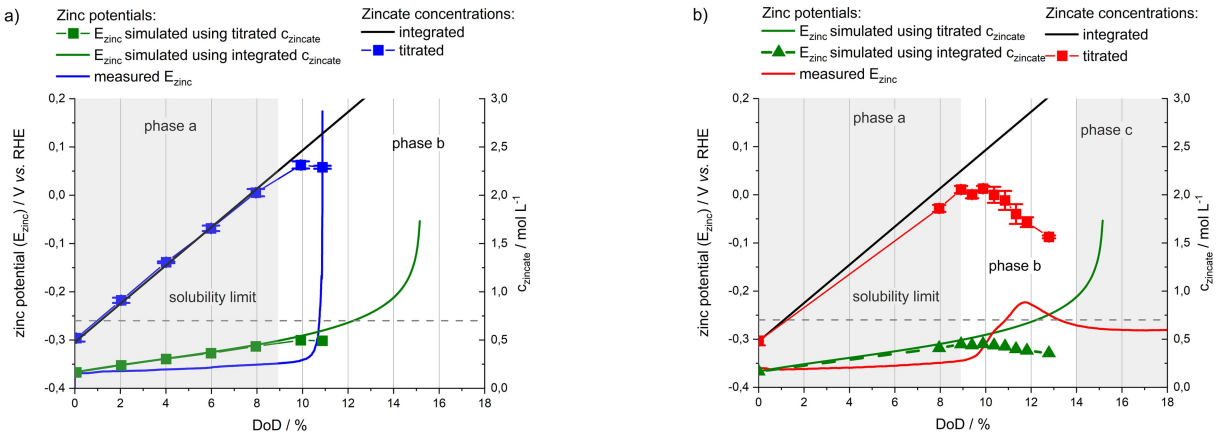

Figure 4. Measured (blue and red boxes, titrated) and calculated (black line) zincate concentration in the liquid phase of the slurry anode and potential of the zinc electrode of a zinc-air flow cell during galvanostatic discharge with 50 mA cm^{-2} (blue line), and 16 mA cm^{-2} (red line), slurry electrode with 50 wt.-% zinc, 7 mol L^{-1} KOH and 0.48 mol L^{-1} ZnO, room temperature, cut-off criterion cell voltage <0.4 V, black line shows the values, calculated from the transferred charge for an oxidation where zincate is the only product, green curves were calculated using Equation 2 (lines using integrated, boxes and triangles using titrated zincate concentrations).

Our data shows that a sufficiently high rate of Equation 1-2 can only be achieved via a sufficiently high ZnO surface area. At too high current densities, the critical zincate concentration is reached before the ZnO surface area had sufficient time to grow.

The nucleation process of ZnO itself is complicated: ZnO seeding crystals were shown to not accelerate ZnO precipitation.[16] Debiemme-Chouvy et al,[41] on the other hand, found an effect of ZnO seeding crystals, but only at timescales >100 h. In our experiments, there are only about half an hour (100 mA cm^{-2}) and 1 h (50 mA cm^{-2}) between reaching the supersaturation described by Debiemme-Chouvy et al[41] and passivation. In our electrolytes, the homogeneous precipitation of ZnO did not happen during discharge, but about half an hour after cell failure. The nucleation of the ZnO in the bulk of the electrolyte came too late to affect the discharge.

We therefore conclude that the rate determining step is the nucleation and growth of the ZnO in the bulk of the electrolyte. Once ZnO particles offer sufficient overall surface area to capture zincate at a rate higher than the electrochemical zincate formation, they are able to reduce the zincate concentration and keep it at a sufficiently low level. In this case, phase b is not the end of discharge and transitions into phase c. Higher KOH-concentrations come with much slower ZnO precipitation,[41] which explains why none of our measurements with 12 mol L^{-1} KOH reached phase c (Figure 2b).

Phase c

When reached, this phase of discharge starts between 11 and 12% DoD (at a zincate concentration of approx. 2.1 mol L^{-1}) and lasts until cell failure due to slurry solidification. The decreasing measured zincate concentration at the beginning shows that the ZnO precipitation rate is higher than the zinc oxidation rate. After the initial decrease, the zincate concentration remains roughly stable between approx. 1.4 and 2.1 mol L^{-1} and does not show any reproduceable trends. Most of the ZnO precipitation occurs in the bulk of the electrolyte, so the type I ZnO layer on the zinc particles remains too thin to hamper the diffusion of OH^--ions and cause passivation. Instead, the cell fails due to slurry solidification.

Cell Voltage: Influence of Zincate Concentration

Our titrated zincate concentrations offer the unique opportunity to distinguish between thermodynamic and kinetic contributions to the cell voltage. Kinetic contributions to the overpotential change with the active (non-passivated) surface area of the zinc electrode, which will be discussed in more detail below.

The thermodynamic contributions can be estimated based on the ion concentrations, according to literature:[42–44]

$$\eta_a = \Delta\Phi_a - \Delta\Phi_a^0 - \frac{RT}{zF} * \ln\left(\frac{c_{OH^-}^4}{c_{Zn(OH)_4^{2-}}^1 * c_{std}^3}\right) \quad (2)$$

$\Delta\Phi_a$ is the potential difference between anode and electrolyte, $\Delta\Phi_a^0$ is the open circuit half-cell potential at standard conditions, R, T, z and F are the universal gas constant, the temperature (298 K), the number of exchanged electrons (2) and the Faraday- constant. c_{OH^-}, and c_{std} denote the hydroxide concentration, the zincate concentration and the zincate reference concentration (1 mol L^{-1}), respectively. We assume that the pumped slurry setting implies spatially homogeneous concentrations within the cell.

We simplified the calculations by assuming that $\Delta\Phi_a$ and $\Delta\Phi_a^0$ are constant and adding $\Delta\eta_a$ to the first measured equilibrium zinc potential. The zincate concentrations were either calculated via the Faraday equation and the transferred charge or measured by titration. c_{OH^-} was calculated according

to the reaction in Equation 1-1 by subtracting twice the zincate concentration from the initial KOH concentration.

Figure 4 shows the results of these calculations, as well as the measured zinc potential and the measured zincate concentration.

Phase a

The simulated curves show a continuous increase, until at a DoD of approx. 15% the vanishing OH^--concentration causes a steep increase of the zinc electrode potential. There is little difference between the simulation using the integrated (green line) and the titrated zincate concentration (green boxes and triangles). This is because titrated and integrated zincate concentrations match very well (see discussion after Figure 3). The measured zinc potentials (red and blue lines) increase with a visibly lower slope than the calculated ones. Such a deviation from a simple concentration-based Nernst equation (e.g., Equation 2) was reported by many other groups,[16,35,45–48] but with different explanations. Hampson et al[35] claim that there must be different zinc species in solution. These zinc species are probably polynuclear, e.g. $Zn_2O_2(OH)_2^{4-}$,[16] and therefore need fewer than 4 OH^--ions. Zelger et al[47] postulate concentration dependent activity coefficients (which are one in Equation 2). Another group[35] concludes, that above the solubility limit transparent colloids are formed. These transparent colloids have been described by other authors as well.[3] Our opaque system does not allow in situ speciation analysis, we therefore cannot determine the contribution of the different effects to the potential of the zinc electrode.

Phase b

During this phase, the cell passivates, or in case of current densities of 20 $mA\,cm^{-2}$ or lower, the zincate concentration decreases due to ZnO precipitation. The simplified concentration-based overpotential model (Equation 2) neglects ZnO precipitation, hence the simulation predicts a steep potential increase at a DoD of ∽15%, due to depletion of OH^--ions, which is approx. 4% DoD later than measured.

The comparison of the measured zincate concentration (blue and red boxes) and the measured zinc potential (blue and red curve) shows that during the steep increase of the zinc potential, the zincate concentration remains constant or is even decreasing. Moreover, at low current densities (16 $mA\,cm^{-2}$, Figure 4 b) the potential of the zinc electrode continues to increase until a DoD of 12%, even though the measured zincate concentration is stationary or declining. This declining zincate concentration decreases the calculated potential in Figure 4b by approx. 15 mV, which is much less than the measured approx. 50 mV. Therefore, the zincate concentration cannot be the reason for the increasing potential of the zinc electrode. Otherwise, the two graphs would have the maximum values at the same DoD. This behavior indicates that the voltage changes in phases b and c are not dominated by ion concentrations (Nernstian, see Equation 2), but rather by passivation-related kinetic overpotentials.

Phase c

In phase c, cell voltage and zinc electrode potential increase and decrease, respectively (see Figure 2). The zincate concentrations scatter in a wide range (1.4 to 2.1 $mol\,L^{-1}$) without any apparent correlation to the zinc electrode potential (see Figure 3). Therefore, the zincate concentration has a negligible effect on the cell voltage in this regime.

Kinetic Overpotentials and passivation

Although passivation is frequently described as an effect which is caused by a certain (critical) zinc potential,[19–23] it also may influence the zinc potential via the Tafel equation.[49] A decreasing active area combined with a constant total current lead to increasing effective current densities, which cause higher overpotentials and a logarithmic increase of the electrode potential. We see this as the root cause for the steep increase of the zinc potential at the beginning of phase b.

Right from the beginning of discharge, zinc dissolution occurs via pitting (see Figures S1 and S2 or[50]).

This creates fresh zinc surface area, to which we attribute the recovery of the cell voltage in phase b and c, which only occurs at low current densities. Interestingly, we do not see an effect of the current density on the zinc potential in phase a. We suggest that mass transport rather than electrochemical kinetics dominates the overpotential in phase a. The key towards discharging beyond the supersaturation limit, i.e. reaching phase c, lies in a sufficiently high precipitation rate of ZnO. This reaction decreases the zincate concentration, and it is governed by the ZnO surface area created so far.

A toy Model

Figure 5 illustrates our working hypothesis in more detail. At the beginning of discharge, the zinc particles are covered by an incomplete passivation layer, probably resulting from the exposure of the particles to air. During the first phase of discharge zinc dissolution occurs via pitting[50] (phase a). Since the zinc particles are only temporarily connected to the current collector (pumping replaces the slurry every 7 seconds), no pronounced concentration gradients develop between a particle and the surrounding solution.

Once the critical zincate concentration is reached, passivation starts. It is widely accepted that the passivating type II ZnO forms as discrete nuclei which grow until they eventually coalesce and cover the whole surface of the electrode.[19–23] In phase b, this effect has decreased the active area so far that it measurably increases the zinc potential (Tafel equation).[51]

At low current densities, the nucleation of ZnO in the bulk of the solution is fast enough to decrease the zincate

Research Article
doi.org/10.1002/batt.202400298
Chemistry Europe
European Chemical Societies Publishing

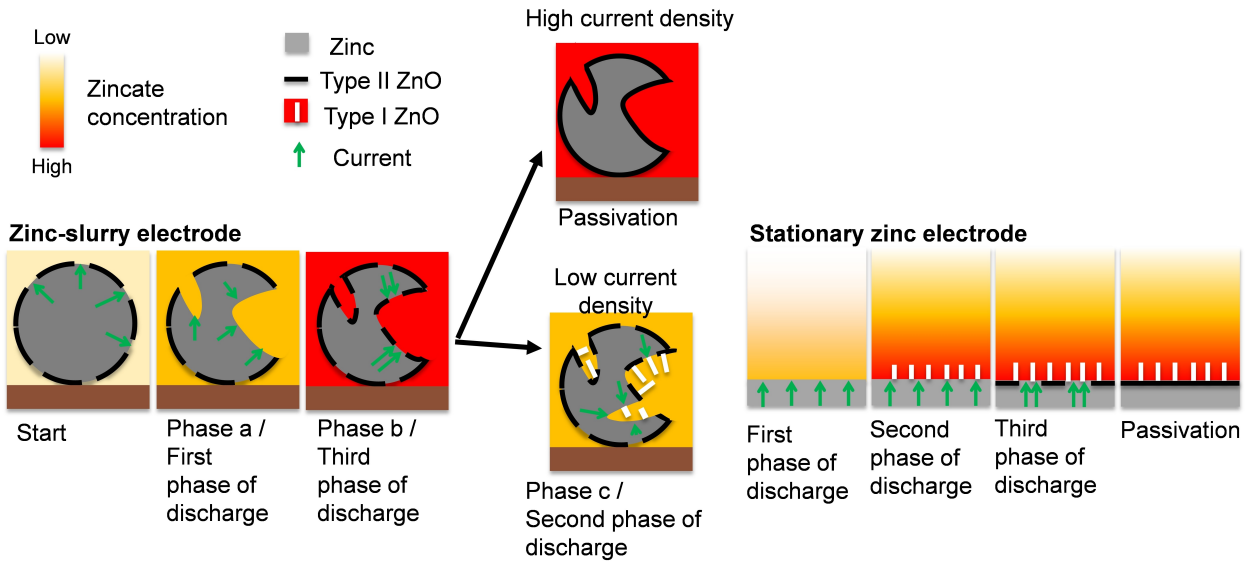

Figure 5. Schematic representation of the proposed discharge mechanism (stationary zinc electrode according to[23]).

concentration before the electrode is fully passivated. At high current densities this effect is negligible and the electrode passivates completely. As the electrolyte is supersaturated (> 300 %) with ZnO, it is unlikely that the recovery is due to the dissolution of the passivating layer. Instead, it is probably due to an increase of the active area by pitting, just like at the beginning of discharge. All zinc particles remain active, because at higher DoDs (30–40 %) all zinc particles are much more corroded than at a DoD of 12 % (see supplementary information, Figure S2). The decreasing zincate concentrations hardly contribute to the recovery of the zinc potential, because during phase a, the potential of the zinc electrode was hardly sensitive to the zincate concentration.

In this scenario, the increasing potential is a symptom of passivation and not its cause, which is in contrast to references.[19–23] Our measurements indicate that the active area of the zinc electrode shows a local minimum at a DoD of approx. 12 % before it starts to increase again. This increase shows that the passivation reaction becomes negligible at an overpotential approx. 0.15 V higher than at the onset of passivation. So, despite the fact that passivation always starts at the same potential, this potential is not the reason for passivation and therefore not critical.

This effect was never noticed before, because stationary electrodes show several important differences compared to the slurry electrode which was used in this study, as shown in Figure 5. The main differences are that stationary electrodes always show a concentration gradient, because even in fast flowing electrolytes there is a thin, immobile electrolyte layer directly at the surface of the electrode,[49] and the bulk zincate concentration is roughly stable due to the large amount of electrolyte used. The nucleation of ZnO occurs therefore at the zinc surface only, and usually much earlier than in our system, e.g..[23] This ZnO restricts the diffusion of zincate and OH^--ions and eventually causes passivation.[15,23] Declining zincate concentration in the bulk of the electrolyte therefore would not reach the surface of the zinc electrode, so it is not possible to change the zincate concentration at the surface of the electrode after the start of the passivation process.

Critical Zincate Concentration

Our observations indicate a critical zincate concentration that depends on the KOH concentration of the electrolyte (2.3 mol L^{-1} for both measurements with 7 mol L^{-1} KOH and 3.7 mol L^{-1} in 12 mol L^{-1} KOH, see Figure 3). As the electrodes in all experiments depicted in Figure 2 b (six measurements with 7 mol L^{-1} KOH and three measurements with 12 mol L^{-1} KOH) passivate at approx. the same DoD, we conclude that the zincate concentration at the point of passivation does not depend on the current density but only on the KOH concentration.

There is a set of theories, which identifies a critical zincate concentration as the starting point of passivation.[15,24–27,52] These theories are based on the work of Marshall et al.[25] and Hampson et al..[27] These groups did not measure the zincate concentration itself, but the passivation charge[25] or passivation time[27] at different KOH and initial zincate concentrations. They found a linear correlation between passivation time/charge and initial zincate concentration. They used this correlation to calculate the zincate concentration at zero passivating charge/time. This concentration was always equal to half the KOH concentration, so they claimed that the critical zincate concentration can be estimated by dividing the KOH concentration by two. The postulated reason was that this is the point when there are insufficient OH^--ions to produce zincate (according to Equation 1-1). Our critical zincate concentrations, however, are lower than predicted by this formula, i.e., the OH^--concentration is not even close to zero: according to our measured zincate

concentrations, there are at least 2 mol L^{-1} of OH^- in 7 mol L^{-1} KOH and 4 mol L^{-1} of OH^- in 12 mol L^{-1} KOH left at the point of passivation. A similar behavior can be found in the data presented in refs.[26,33]

We see three potential causes for the predominant surface passivation pathway (according to Equation 1-3). The desired zincate pathway (Equation 1-1) may become slower than the surface passivation pathway because of an insufficient activity of the OH-ions, a too high activity of the zincate, or an insufficient water activity. In our system, all three activities are linked to the zincate concentration, so our data do not allow to distinguish between these scenarios.

As to OH^-, it is important to highlight, that its activity is much higher at the point of passivation in 12 than in 7 mol L^{-1} KOH (4 instead of 2 mol L^{-1} OH^-). This makes the OH^--activity an unlikely sole reason for passivation. Nevertheless, the passivating charge (DoD) is also higher in 12 mol L^{-1} KOH, which shows that a high activity of OH^--ions favors Equation 1-1. Dirkse et al[52] claim that the diffusion of OH^--ions is much slower in higher concentrated KOH solutions, but if passivation would occur when diffusion is too slow to deliver enough OH^--ions, the passivating charge (DoD of cell failure) would depend on the current density. As Figure 2 b shows that this is not the case, the only explanation left are the different zincate concentrations.

As to zincate concentration, one would have to speculate that a high zincate concentration slows down the forward reaction of Equation 1-1, thus giving Equation 1-3 an upper hand under galvanostatic conditions. On the other hand, it might only bind water in its hydration shell.

As to water, it represents a hidden reactant of Equation 1-1 which is however crucial to stabilize the dissolved zincate. With increasing DoD more water is bound in solvation shells, which again might favor Equation 1-3 over Equation 1-1. At 12 mol L^{-1} KOH, less water is available because it is bound in the KOH solvation shells, which might explain the higher OH^--concentration at the point of passivation.

As literature shows, that the passivating charge is influenced by KF (which binds water, but does not affect OH^- or zincate concentration), water has to play a role in the passivating process.[52–53] It cannot be the sole reason for passivation, because many groups showed that a high KOH concentration increases the passivating charge,[25,27,48] even when the KOH has consumed all water for its hydration shell.

We conclude that none of the three activities is the sole reason for passivation. Instead, all of them influence the point of passivation.

Overcoming passivation and reaching phase c, is only possible when ZnO precipitation (Equation 1-2) reaches a sufficiently high rate. This seems to demand the availability of ZnO growth areas, which in turn are exclusively on ZnO nuclei from Equation 1-2. Their growth is inherently slow, so phase c is only reached at low current densities. In 12 mol L^{-1} KOH, this process is even slower than in 7 mol L^{-1} KOH, probably because of a higher ZnO solubility, so phase c was never reached in our experiments.

Conclusions

The pumped zinc-slurry anode used in this work offers several unique insights into the zinc electrochemistry. It allows in-operando measurements of the zincate concentration, which is crucial for understanding the passivation process and the potential curve.

The discharge occurs in two or three phases (a,b,c). During phase a, zincate is the only (high current densities) or main (low current densities) oxidation product. The cell voltage steadily drops, dominated by an apparently Nernstian behavior. However, the version of the Nernst equation used in recently published models of zinc electrodes, overestimates the concentration dependent overvoltages. We could not determine the reason for this behavior, it may be due to decreasing activity coefficients or the formation of less active zinc species (polynuclear or colloidal).

Phase b starts at a DoD of approx. 11 % ($\approx$90 mAh g_{zinc}^{-1}), where the cell voltage drops steeply. This drop cannot be Nernstian, because the zincate concentration remains stable and there is no depletion of OH^--ions. Therefore, it has to be a kinetic effect caused by growing kinetic barriers due to Zn particle surface passivation.

In contradiction to some publications, passivation is not due to a critical zinc potential: Although the passivation process always starts at the same potential, passivation may (at low currents, see phase c) stop at an overvoltage which is approx. 0.15 V higher than at the onset of passivation. If a critical zinc potential was the root cause for passivation, this would be impossible.

In our system, passivation occurs at a certain (titrated) zincate concentration. This zincate concentration is directly linked to the activities of OH^- and water. We propose that the passivation process is determined by more than one of these three activities/concentrations, because the critical zincate concentration and the remaining OH^--concentration depends on the KOH-concentration.

Phase c is only reached at slow (low current) discharge. It follows a voltage drop to a local minimum in phase b. The increasing voltage reflects an increasing active area of the zinc electrode, because the zincate concentration does not show a corresponding trend.

Slow operation keeps the zincate concentration under the critical limit, because homogeneous nucleation of ZnO (crystallites unattached to zinc particles) occurs. These crystallites act as catalysts and increase the ZnO precipitation speed and consume zincate until a steady state is reached. At 12 mol L^{-1} KOH concentration this effect is too slow to prevent passivation.

High ZnO solubility, as achieved via high KOH concentrations, is a double edged sword: it elongates phase a, but at a too high KOH concentration may prevent reaching phase c. As phase c is longer than phase a, higher KOH concentrations may actually decrease the DoD of cell failure.

Even at slow operation, discharge eventually ends when the slurry is mechanically blocked by its own growing viscosity. The

cell then discharges as one would expect for a static zinc-powder based zinc-air cell.

The achieved specific capacity of 460 $Ah\,L_{slurry}^{-1}$ is considerably higher than the 240 $Ah\,L^{-1}$ reported in literature. Our next aim will be looking for additives which can optimize the ZnO nucleation process to achieve these high specific capacities at higher current densities.

Acknowledgements

This work was supported by the German Federal Ministry for Economic Affairs and Climate Action during the ZnMobil project (grant number 03ET6090F). We also thank our project partners Grillo-Werke AG and Covestro Deutschland AG for supplying chemicals and air electrodes. We also want to thank Azelis for providing separator product samples and the Westfälischen Hochschule for the SEM-measurements. Open Access funding enabled and organized by Projekt DEAL.

Conflict of Interests

The authors declare no conflict of interest.

Data Availability Statement

The data that support the findings of this study are available from the corresponding author upon reasonable request.

Keywords: zinc-air flow batteries · zinc passivation

[1] K. Harting, U. Kunz, T. Turek, *Z. Phys. Chem.* **2012**, *226*, 151–166.
[2] B. Amunátegui, A. Ibáñez, M. Sierra, M. Pérez, *J. Appl. Electrochem.* **2018**, *48*, 627–637.
[3] A. J. Appleby, M. Jacquier, *J. Power Sources* **1976**, *1*, 17–34.
[4] S. Smedley, *IEEE AESS* **2000**, *15*, 19–22.
[5] S. I. Smedley, X. G. Zhang, *J. Power Sources* **2007**, *165*, 897–904.
[6] S. Smedley, W. Tivy, B. Wozniczka, D. R. Bruce, US Patent 10,826,142, **2020**.
[7] H. Baba, *SAE Trans.* **1971**, *80*, 930–936.
[8] J. Cooper, *Sci. Technol. Rev.* **1995**, *10*, 7–13.
[9] J. F. Cooper, University of California, US 5,434,020, **1995**.
[10] N. J. Cherepy, R. Krueger, J. F. Cooper, in *Fourteenth Annual Battery Conference on Applications and Advances.* Proceedings of the Conference (Cat. No.99TH8371), **1999**, pp. 11–13.
[11] J. W. Evans, G. Savaskan, *J. Appl. Electrochem.* **1991**, *21*, 105–110.
[12] G. Savaskan, T. Huh, J. W. Evans, *J. Appl. Electrochem.* **1992**, *22*, 909–915.
[13] M. Bockelmann, U. Kunz, T. Turek, *Electrochem. Commun.* **2016**, *69*, 24–27.
[14] F. Mahlendorf, A. Heinzel, C. Müller, D. Fuchs, in *Electrochemical Power Sources: Fundamentals, Systems, and Applications: Metal–Air Batteries*: Present and Perspectives (Eds.: H. Arai, J. Garche, L. Colmenares), Elsevier, **2020**, pp. 99–123.
[15] M. B. Liu, G. M. Cook, N. P. Yao, *J. Electrochem. Soc.* **1981**, *128*, 1663–1668.
[16] T. P. Dirkse, *J. Electrochem. Soc.* **1981**, *128*, 1412–1415.
[17] M. Bockelmann, L. Reining, U. Kunz, T. Turek, *Electrochim. Acta* **2017**, *237*, 276–298.
[18] A. Hugot-Le Goff, S. Joiret, B. Saidani, R. Wiart, *J. Electroanal. Chem. Interfacial Electrochem.* **1989**, *263*, 127–135.
[19] M. Hull, J. Ellison, J. Toni, *J. Electrochem. Soc.* **1970**, *117*, 192.
[20] R. W. Powers, M. W. Breiter, *J. Electrochem. Soc.* **1969**, *116*, 719–729.
[21] R. Armstrong, G. Bulman, *J. Electroanal. Chem. Interfacial Electrochem.* **1970**, *25*, 121–130.
[22] M. Mokaddem, P. Volovitch, K. Ogle, *Electrochim. Acta* **2010**, *55*, 7867–7875.
[23] M. Bockelmann, M. Becker, L. Reining, U. Kunz, T. Turek, *J. Electrochem. Soc.* **2018**, *165*, A3048–A3055.
[24] N. Hampson, P. Shawt, R. Taylor, *Br. Corros. J.* **1969**, *4*, 207–211.
[25] A. Marshall, N. A. Hampson, *J. Appl. Electrochem.* **1977**, *7*, 271–273.
[26] A. Marshall, N. A. Hampson, M. P. Saunders, J. S. Drury, *J. Electroanal. Chem. Interfacial Electrochem.* **1977**, *78*, 307–311.
[27] N. A. Hampson, P. E. Shawt, R. Taylor, *Br. Corros. J.* **1969**, *4*, 207–211.
[28] T. P. Dirkse, N. A. Hampson, *Electrochim. Acta* **1972**, *17*, 387–394.
[29] R. W. Powers, *J. Electrochem. Soc.* **1971**, *118*, 685.
[30] E. Farmer, A. Webb, *J. Appl. Electrochem.* **1972**, *2*, 123–136.
[31] S. Hosseini, S. J. Han, A. Arponwichanop, T. Yonezawa, S. Kheawhom, *Sci. Rep.* **2018**, *8*, 11273.
[32] S. Hosseini, W. Lao-atiman, S. J. Han, A. Arpornwichanop, T. Yonezawa, S. Kheawhom, *Sci. Rep.* **2018**, *8*, 14909.
[33] M. Eisenberg, H. Bauman, D. Brettner, *J. Electrochem. Soc.* **1961**, *108*, 909.
[34] A. Marshall, N. A. Hampson, J. S. Drury, *J. Electroanal. Chem. Interfacial Electrochem.* **1975**, *59*, 19–32.
[35] N. Hampson, G. Herdman, R. Taylor, *J. Electroanal. Chem. Interfacial Electrochem.* **1970**, *25*, 9–18.
[36] R. J. Gilliam, J. W. Graydon, D. W. Kirk, S. J. Thorpe, *Int. J. Hydrogen Energy* **2007**, *32*, 359–364.
[37] V. Rezaite, L. Deresh, *Prot. Met.* **2006**, *42*, 334–338.
[38] T. P. Dirkse, in *Copper, Silver, Gold & Zinc, Cadmium, Mercury Oxides & Hydroxides* (Ed.: T. P. Dirkse), Pergamon, Amsterdam, **1986**, p. 162.
[39] T. P. Dirkse, N. A. Hampson, *Electrochim. Acta* **1972**, *17*, 135–141.
[40] T. J. Petek, N. C. Hoyt, R. F. Savinell, J. S. Wainright, *J. Electrochem. Soc.* **2016**, *163*, A5001–A5009.
[41] C. Debiemme-Chouvy, J. Vedel, *J. Electrochem. Soc.* **1991**, *138*, 2538–2542.
[42] J. Stamm, A. Varzi, A. Latz, B. Horstmann, *J. Power Sources* **2017**, *360*, 136–149.
[43] E. Deiss, F. Holzer, O. Haas, *Electrochim. Acta* **2002**, *47*, 3995–4010.
[44] W. Lao-Atiman, K. Bumroongsil, A. Arpornwichanop, P. Bumroongsakulsawat, S. Olaru, S. Kheawhom, *Front. Energy Res.* **2019**, *7*, 15.
[45] T. P. Dirkse, N. A. Hampson, *Electrochim. Acta* **1971**, *16*, 2049–2056.
[46] C. G. Smith, PhD thesis, California Univ., Berkeley, **1978**.
[47] C. Zelger, M. Süßenbacher, A. Laskos, B. Gollas, *J. Power Sources* **2019**, *424*, 76–81.
[48] M. Bockelmann, M. Becker, L. Reining, U. Kunz, T. Turek, *J. Electrochem. Soc.* **2019**, *166*, A1132–A1139.
[49] C. Hamann, W. Vielstich, in Elektrochemie, Wiley-VCH, Weinheim, p. 168.
[50] D. Fuchs, PhD thesis, University Duisburg-Essen, **2021**.
[51] A. Rinaldi, O. Wijaya, H. E. Hoster, *ChemElectroChem* **2016**, *3*, 1944–1950.
[52] T. Dirkse, D. Kroon, *J. Appl. Electrochem.* **1971**, *1*, 293–296.
[53] T. P. Dirkse, N. A. Hampson, *Electrochim. Acta* **1972**, *17*, 813–818.

Manuscript received: May 2, 2024
Revised manuscript received: May 29, 2024
Accepted manuscript online: June 25, 2024
Version of record online: August 9, 2024